We are IntechOpen, the world's leading publisher of Open Access books Built by scientists, for scientists

4,800
Open access books available

122,000
International authors and editors

135M
Downloads

Our authors are among the

154
Countries delivered to

TOP 1%
most cited scientists

12.2%
Contributors from top 500 universities

CLARIVATE ANALYTICS BOOK CITATION INDEX INDEXED

WEB OF SCIENCE™

Selection of our books indexed in the Book Citation Index in Web of Science™ Core Collection (BKCI)

Interested in publishing with us?
Contact book.department@intechopen.com

Numbers displayed above are based on latest data collected.
For more information visit www.intechopen.com

3

Anisotropy of Light Extraction Emission with High Polarization Ratio from GaN-based Photonic Crystal Light-emitting Diodes

Chun-Feng Lai[1], Chia-Hsin Chao[2], and Hao-Chung Kuo[1]
[1]*Department of Photonics and Institute of Electro-Optical Engineering, Nation Chiao-Tung University*
[2]*Electronics and Opto-Electronics Research Laboratories, Industrial Technology Research Institute*
Hsinchu, Taiwan, Republic of China

1. Introduction

1.1 General background

GaN-based materials have been attracted a great deal of attention due to the large direct band gap and the promising potential for the optoelectronic devices, such as light emitting diodes (LEDs) and laser diodes (LDs). LEDs have the advantages of small size, conserve energy, and have a long lifespan. LEDs of solid-state lighting will be in a position to replace conventional lighting sources within years. At present, the efficiency of LEDs is still lower than that of fluorescence lamps in general lighting applications. Therefore, the ultimate optimization of all aspects of LED efficiency is necessary in solid-state lighting development. Several factors are likely to limit the light extraction efficiency of LEDs. One may think that the main limiting factor is internal light generation as internal quantum efficiency (IQE). Nevertheless, this is not the case in a variety of material where the conversion from carriers to photons reaches 50% to 90% if the material's quality is high enough. In this case, the strongest limiting factor is that of external extraction efficiency, i.e. the ability for photons generated inside the semiconductor material to escape into air. Unfortunately, most of the light emitted inside the LED is trapped by total internal reflection (TIR) at the material's interface with air. Although many efficient light extraction strategies have already been applied, they are mostly based on the principle of randomizing the paths followed by the light, such as surface roughening [1-2], flip-chip [3-4], and photonic crystals (PhCs) [5-6].

1.2 Research niche

Light-emitting diodes (LEDs) have become ubiquitous in illumination and signal applications as their efficiency and power level improve. While the improvement of the basic characteristics will benefit the replacement of the conventional light sources, further improvement in other characteristics can bring about unique applications. One notable example is the polarized light emission which is highly desirable for many applications [7],

Source: Recent Optical and Photonic Technologies, Book edited by: Ki Young Kim,
ISBN 978-953-7619-71-8, pp. 450, January 2010, INTECH, Croatia, downloaded from SCIYO.COM

e.g. back-lighting for liquid crystal displays and projectors. For the application of next-generation LEDs, such in projector displays, backlight displays, and automobile headlights, further improvements the light extraction efficiency, the polarized emission, and the directional far-field patterns of light sources are required. Recently, PhC has attracted much attention for the possibility to improve the extraction efficiency [8-9], polarization [10], and directional far-field patterns [11-12] from GaN-based LEDs and GaN-based film-transferred LEDs, respectively. In order to optimize the PhC LED performance for a specific system, detailed knowledge of the light extraction and polarization, especially the angular distribution, is required. The light wave propagating in the PhC LED waveguide, with its propagation partially confined by the TIR, can interact with the reciprocal lattice vectors of the two-dimensional (2D) PhC lattice to exhibit a variety of novel behaviors from the light localization. On the other hand, through the Bragg diffraction with the PhC which fabricated on LEDs can scatter the guided light into the escaping cone to circumvent the deleterious effects due to TIR, which traps the majority of the emitted light in LED chips. In this study, the GaN-based LEDs with PhCs were demonstrated and investigated in the light extraction, and polarization.

In this chapter, we first introduce the theory analysis and design method of GaN-based PhC LED structures in section 2. Then, in section 3, we exhibit the direct imaging of the azimuthal angular distribution of the 2D PhC light extraction using a specially designed waveguide structure. The optical images of the light extraction patterns from the guided electroluminescence (EL) light are obtained with a current injected into the center of the annular structure made on the GaN multilayer. With increasing lattice constant, symmetric patterns with varying number of petals according to the symmetry of the PhC are observed. The observed anisotropy is charted using the Ewald construction according to the lattice constant and the numerical aperture of the observation system. The appearance and disappearance of the petals can be explained using the Ewald construction in the reciprocal space. In addition, several novel features of light propagations associated with the PhC can also be directly observed including the focusing and collimating behavior. These results can be used for the optimization of LED devices with PhC extraction. Next, in section 4, polarization characteristics of the GaN-based PhC LEDs using an annular structure with square PhC lattice have been studied experimentally and theoretically. The observed a strong polarization dependence of the lattice constant and orientation of the PhC. It is found that the PhC can be as a polarizer to improve the *P/S* ratio of the extracted EL emission. The results of the *P/S* ratio for light propagating in different lattice orientation were found to be consistent with the results obtained using the PhC Bloch mode coupling theory. This polarization behavior suggests an efficient means to design and control the GaN blue PhC LEDs for polarized light emission. Finally, conclusions are provided in section 5.

2. Fundamental and modelling of photonic crystal LEDs

2.1 Waveguide properties of LED structures

Although the IQE of GaN-based LEDs have reached up to 90%, the light emission from a multi-quantum well (MQW) into the air is fundamentally limited by TIR. LEDs have such low external extraction efficiency that most of the light generated in a high-index material is trapped by TIR. Due to the GaN-based LED layer behaving as a waveguide, trapped light is distributed in a series of so-called guided modes. The propagation properties, including electromagnetic field distributions and wave vectors of guided modes, affect PhC light

extraction behavior. In general, the high order guided modes interact strongly with PhC to have high extraction efficiency. By contrast, the low order guided modes have weak light extraction efficiency due to the poor overlap with the PhC regions. But the light of energy distribution coupling to the low order guided modes is larger. Therefore, our discussion begins with the guided mode properties in a waveguide structure of LED semiconductor layers, which is helpful to optimize the design of PhC structure on LEDs with high light extraction efficiency.

A large number of waveguide modes exist in a typical GaN-based LED structure as asymmetric slab waveguide in geometry. For example, GaN-based blue LED structure is grown by metal-organic chemical vapor deposition (MOCVD) on *c*-sapphire substrate. The GaN blue LED structure consists of a 2 μm-thick un-GaN buffer layer, a 2-μm-thick n-GaN layer, a 100 nm InGaN/GaN MQW region, and a 200 nm-thick p-GaN layer, as shown in Fig. 1(a). In order to study the guided modes in the LED structures, the guided mode distributions were calculated in the asymmetric slab waveguide with the vertical effective refractive index profile, as shown in Fig. 1(b). Since the emitted light from the MQW is predominantly TE polarized in the waveguide plane [13], only TE modes are analyzed. In this case, thirty-two TE guided modes with effective refractive index distribution are obtained by using waveguide theory [14]. The first three and the last of the thirty-two guided modes of electric field distributions are plotted in Fig. 2, respectively. Each guided mode has different electromagnetic field distribution and wave vector. In a planar GaN-based LED on a sapphire substrate, 66% of the total emitted light is wave guided within the GaN layer, while the remainder is found in the delocalized modes in the sapphire, as shown in Fig. 3(a). Only 8.7% of the light generated can directly escape from both top and bottom surfaces of the GaN medium into the air. Further, when the MQW emitter position was be considered in the LED structure, that the guided modes excited a percentage of relative intensity as shown in Fig. 3(b). In the fundamental mode (TE_{00}), the excited percentage is 19.5%; in the other guided modes, the excited percentages are 14.1%, 9.6%, 6.6%, 5.1%, and 3.5%, respectively. The relative intensity ratio of the higher-order modes becomes weak due to the poor field overlap with the MQW emission regions. Therefore, the guided mode energy distribution is mainly in the lower-order modes.

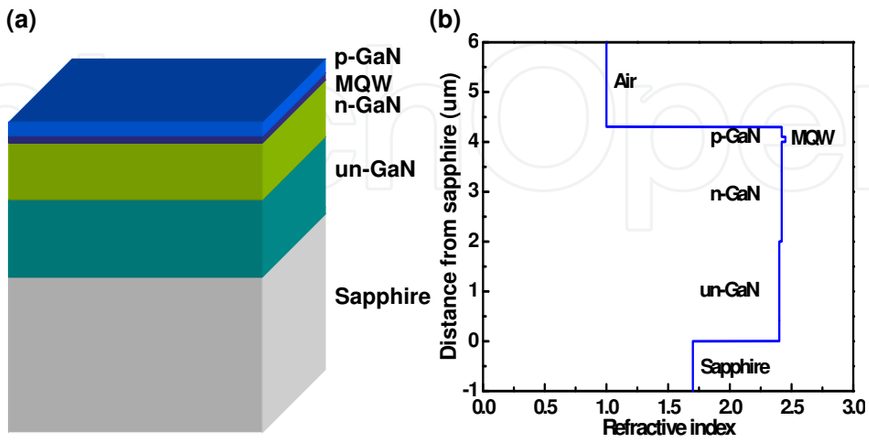

Fig. 1. (a) Schematic diagram of the MOCVD-grown GaN-based blue LED structure (dominant λ = 470 nm). (b) Vertical effective refractive index profile of the characterized GaN-based LED.

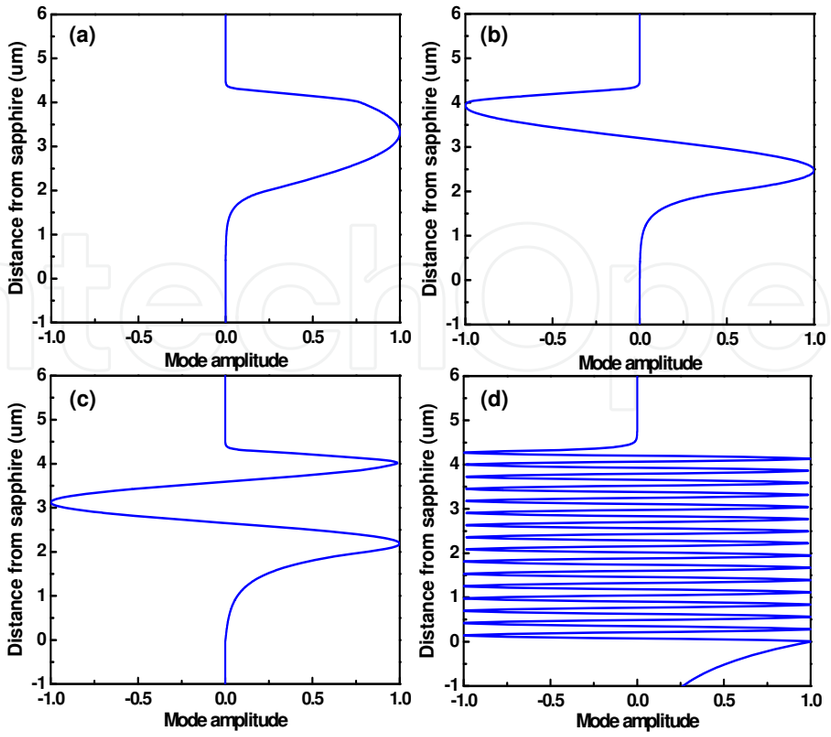

Fig. 2. Electric field distributions of the asymmetric slab waveguide for TE mode are (a) TE_{00} (fundamental mode), (b) TE_{01}, (c) TE_{02}, and (d) TE_{31}.

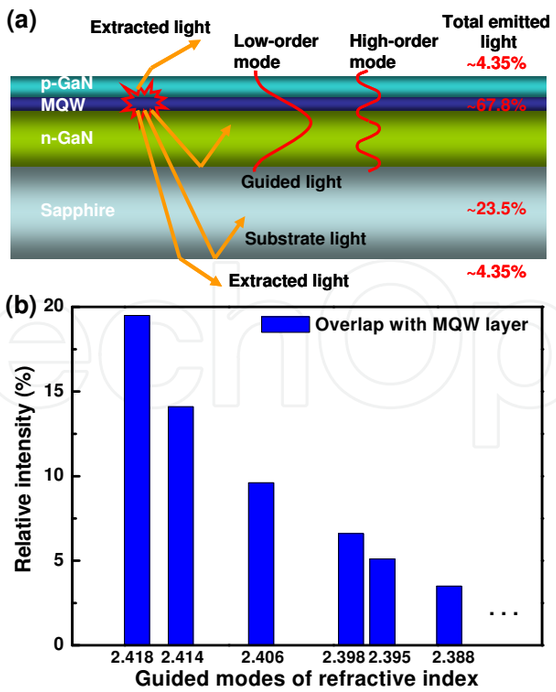

Fig. 3. (a) Possible paths for emitted light in a GaN-based blue LED structure. (b) The guided modes excited percentage of relative intensity indicates overlap with MQW.

2.2 Ewald construction of Bragg's diffraction theoretical analysis methods for photonic crystals

Photonic crystals (PhCs) are artificial structures containing periodic arrangements of dielectric materials which exhibit unique dispersion properties (e.g. such as photonic bandgap (PBG) [15]) and that manipulate light emission behaviors. In this chapter, we will concentrate on the extraction of waveguide light from GaN-based LED structures. There are several schemes to obtain light extraction through PhC nanostructures [16], as shown in Fig. 4, such as (a) inhibition of guided modes emission by PBG, (b) spontaneous emission enhanced in a small cavity by Purcell effect, and (c) emission extraction on the whole surface by leaky mode coupling. Accordingly, the emission region can be deeply etched with a pattern to forbid propagation of guided modes, as shown in Fig. 4(a), and thus force the emitted light to be redirected towards the outside. Defects in PhCs behave as microcavities, as shown in Fig. 4(b), such that the Purcell effect can be excited for spontaneous emission enhancement. Then, light can only escape through leaky modes coupling, as shown in Fig. 4(c). In addition, PhCs can also act as 2D diffraction gratings in slabs or waveguides to extract guided modes to the air and to redirect the emission directions.

The optimal design of PhC structures for high extraction efficiency is promising, which is strongly dependent on various parameters such as lattice constant (a), the type of lattice (square, triangular…), filling factor (f), and etch depth (t). Among parameters described here, we paid special attention to the effect of the lattice constant a. In order to discuss the effect of the lattice constant, we use the Ewald construction of Bragg's diffraction theory. In addition, the plane-wave expansion method (PWE) and the finite-difference time-domain method (FDTD) are implemented to investigate the optical properties of PhC numerically.

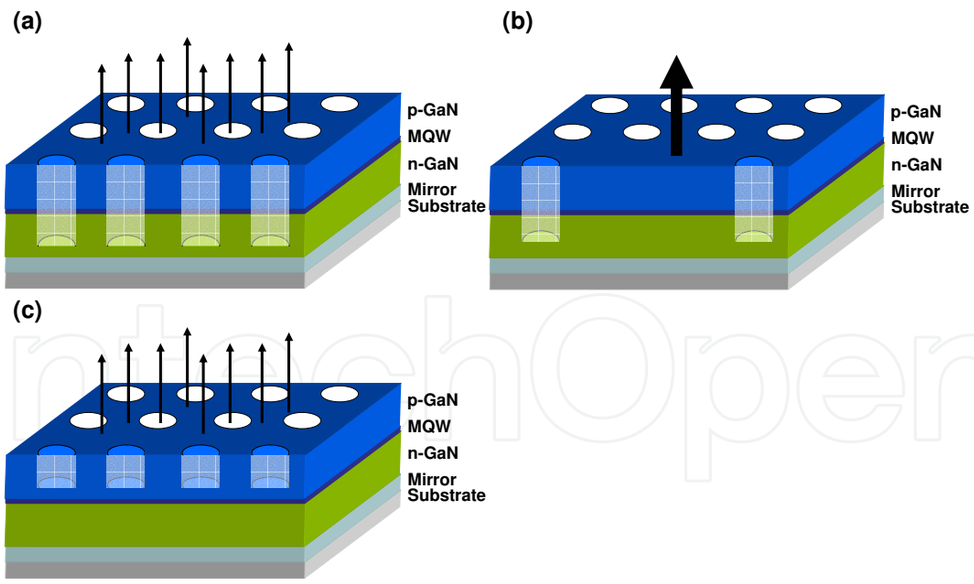

Fig. 4. Schematic the various extraction methods relying on PhCs are (a) PBG, (b) Purcell effect, and (c) leaky mode coupling.

Figure 4(c) is a schematic of the surface grating devices that can be discussed in relation to the light extraction of the lattice constant of PhCs by using the Ewald construction of Bragg's diffraction theorem. The light extraction of guided waves through diffraction by PhC is discussed. According to Bragg's diffraction law, $k_g \sin\theta_1 + mG = k_0 \sin\theta_2$, the phase-matching

diagrams in the wave number space are shown in the Fig. 5(a). The two circles in the Fig. 5 correspond to 1.) the waveguide mode circle with radius $k_g = 2n\pi/\lambda$ at the outside, where n is the effective refractive index of the guided mode; 2.) the air cone with radius $k_o = 2\pi/\lambda$ at the inner circle. The light extraction from PhC also can be quantitatively analyzed using the Ewald construction in the reciprocal space. The extraction of waveguide light into air can be described by the relation $|k_g + G| < k_0$, where G is the diffraction vectors. Such a relation can be represented graphically with the Ewald construction commonly used in the X-ray crystallography. In the present case, for reasons of simplicity, PhC is treated as a 2D in an overall 3D structure as is commonly done. In such case, the reciprocal lattice of the 2D PhC will be represented as the rods protruding perpendicular to the waveguide plane. Figure 5(b) depicts the Ewald spheres for a square lattice with the k vector of the incident light pointing directly at a reciprocal lattice point. The center of the sphere is at the end of the vector and the radius is the magnitude of k_g. The intersection points of the sphere with the protruding rods define the extraction direction of the diffracted light. For simplicity, only the in-plane propagation needs to be treated and a consideration of the projection on the waveguide plane is sufficient. When the in-plane component of the resultant wavevector after the coupling to a reciprocal lattice vector falls inside the air circle, the diffracted light can escape into air, as shown in Fig. 5(c).

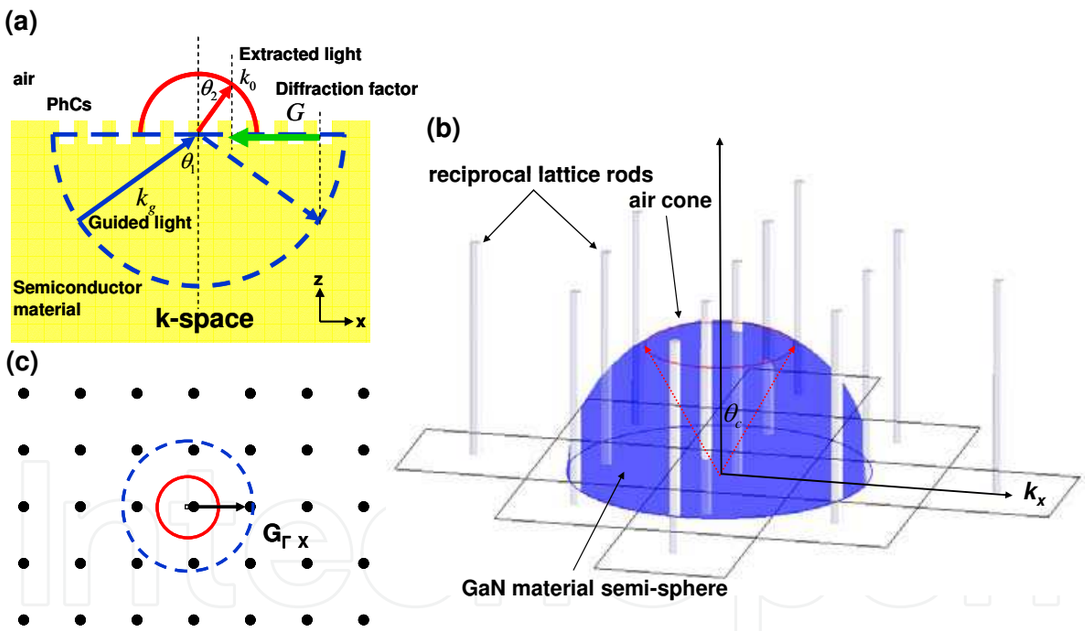

Fig. 5. (a) A schematic of the 2D PhC structure of the Bragg diffraction phase matching diagrams. (b) The Ewald construction for square lattice PhC. (c) The projection of the Ewald sphere construction on the waveguide plane. Thick red circle is air cone and dashed blue circle is waveguide mode cone.

Further, an actual 2D square lattice of PhC as grating has the anisotropy of the diffraction vector [23]. Figure 6 shows the diffraction vector for various lattices constant a, dispersion circles for the in-plane wavevector in air, k_0, and in the semiconductor material, k_g. For example, in the square lattice of PhC, $G_{\Gamma X}$ and $G_{\Gamma M}$ are $2\pi/a$ and $2\sqrt{2}\pi/a$, respectively. When $G_{\Gamma X} > k_0 + k_g$ $[a/\lambda < 1/(n+1)]$, the zone-folded curve does not enter the air curve, so the

diffraction does not occur, as shown in Fig. 6(a). When a is larger than this value, some amount of diffraction occurs, as shown in Fig. 6(b). When a is large enough to satisfy $G_{\Gamma M} < k_0$ ($a/\lambda > \sqrt{2}$), the diffraction vector is wholly included in the air curve, and this gives the maximum light diffraction efficiency. However, the diffraction efficiency cannot be unity for such larger a, since light can find not only the extracted light cone but also another solid angle not extracted by the diffraction. Even in light diffracted into the extracted light cone, half goes downward.

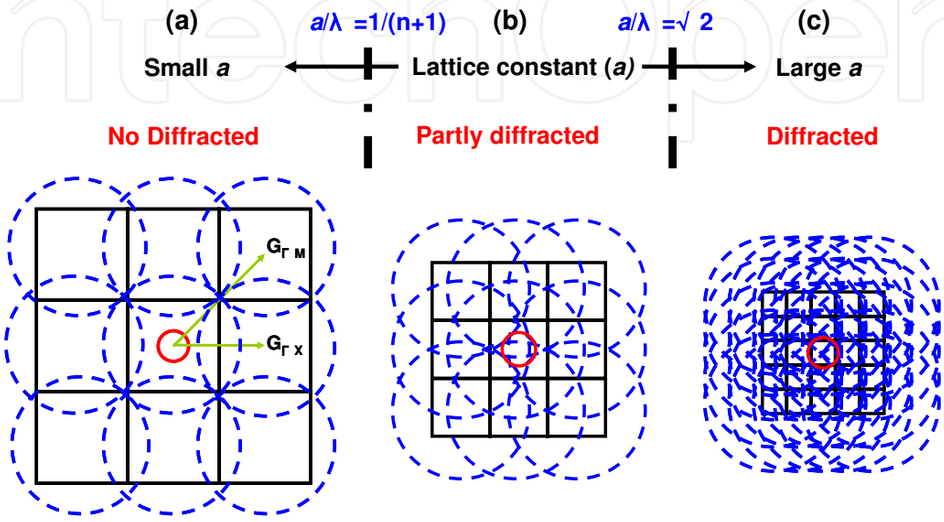

Fig. 6. Brillouin zones for 2D square lattice, dispersion curves of k_0 (center thick red circle) and k_g (dashed blue circle).

3. Anisotropy light extraction properties of GaN-based photonic crystal LEDs

3.1 Sample prepared and measurement results

In order to optimize the PhC LED performance for high light extraction efficiency, detailed knowledge of light extraction is required especially the angular distribution [9, 26]. Therefore, we present the direct imaging of the azimuthal angular distribution of the extracted light using a specially designed annual PhC structure, as shown in Fig. 7(a). The GaN-based LED samples used in this study were grown by metal-organic chemical vapor deposition (MOCVD) on a *c*-axis sapphire (0001) substrate. The LED structure (dominant wavelength λ at 470 nm) was composed of a 1-μm-thick GaN bulk buffer layer, a 2-μm-thick n-GaN layer, a 100-nm-thick InGaN/GaN MQW, and a 130-nm-thick top p-GaN layer. An annular region of square PhC lattice with an inner/outer diameter of 100/200 μm was patterned by holographic lithography. Two different periods of the lattice constant are used by 260 and 410 nm. A scanning electron microscopy (SEM) image of the square-lattice PhC structure is shown inset in Fig. 7(b). The holes were then etched into the top p-GaN layer using inductively coupled plasmon (ICP) dry etching to a depth of t =120 mm. The electron-beam-evaporated Ni/Au film was used as the transparent ohmic contact layer (TCL) to p-GaN, and a 200-nm-thick SiO_2 layer was used for passivation. Finally, Ti/Al/Ti/Au layer was deposited on the n-GaN as an n-type electrode and onto TCL as a p-type electrode on LEDs, respectively. In addition, the schematics for the experimental setup are shown in Fig. 7(b). An electroluminescence (EL) probe station system was utilized for the experiment after

fabrication, which included a continuous wave (CW) current source and a 15x microscope objective with numerical aperture (NA)=0.32. A 15x UV objective with NA of 0.32 was used to collect the on-axis emission signal from the sample, which formed a high-resolution image on a charge-coupled device (CCD); this was recorded with a digital camera. The experiment of the observed image is shown inset in Fig. 7(b).

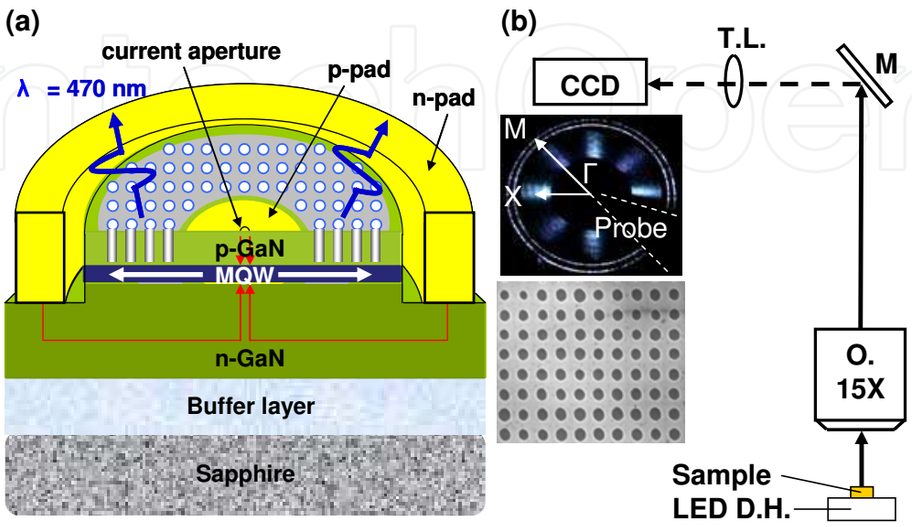

Fig. 7. (a) Schematic diagram of the GaN-based blue LED structure with annular PhC region. (b) EL probe station and CCD imaging system setup, where D.H.:driver holder; M.:mirror; T.L.: tube lens; O.: objective.

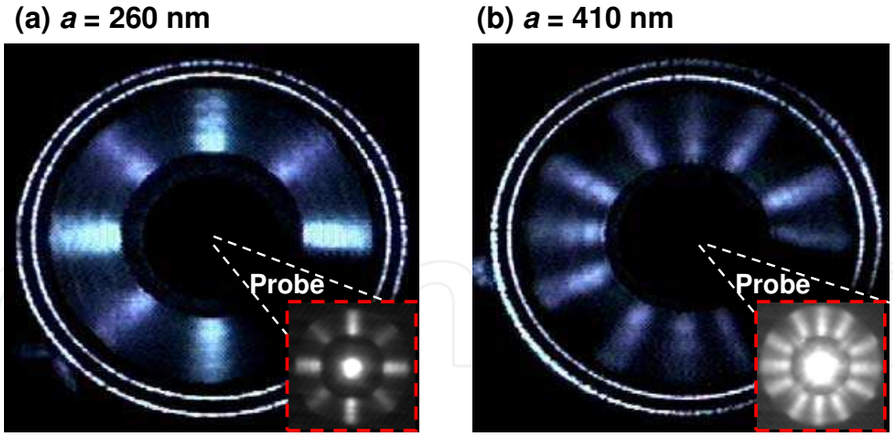

Fig. 8. CCD images taken with square lattices with a = (a) 260 nm and (b) 410 nm. Inset of the photoluminescence (PL) CCD images.

Figure 8 depicts the CCD images for the square PhC structures with lattice constant a of 260 and 410 nm corresponding to a/λ of 0.553 and 0.872, respectively. The EL light was partially guided toward the surrounding PhC region by the waveguide formed by GaN epitaxial layers. This guided light was then coupled into the PhC region and diffracted by the PhC lattice while propagating inside the PhC region. Depending on the lattice constant of the PhC, some of the diffracted light left the wafer and formed the images shown in Fig. 11. It

can be seen that a varying number of petals appears as the lattice constant increases. Under certain conditions, some of the petals may become weaker or disappeared altogether. The observed anisotropy, therefore, primarily arises from the diffraction of guided EL light into the air, which is picked up by the microscope objective.

3.2 Bragg diffraction theoretical discussion

The appearance and disappearance of the petals observed in Fig. 8 can be qualitatively analyzed using the Ewald construction in the reciprocal space. The above observation established that the use of 2D Ewald construction explains the observed images. It can be invoked to determine the boundaries between regions with varying numbers of petals. As shown in Fig. 9, as a/λ increases above the cutoff, the resultant wave vector will start to couple to the shortest lattice vector $G_{\Gamma X}$. The resultant wave vector falls inside the NA circle as shown in Fig. 9(a), where the NA circle with radius NA=0.32k_0 at the inside corresponds to the acceptance angle of the objective lens with NA numerical aperture. For the ΓM direction, the resultant wave vector falls outside the NA circle and will not be seen by the NA=0.32 objective lens as shown in Fig. 9(b). Therefore, a pattern with four petals pointing in the ΓX direction is observed. As a/λ increases further, the resultant wave vector after coupling to $G_{\Gamma X}$ may fall short of the NA circle and therefore it will not be observed, as shown in Fig. 9(c). Thus, there is a range of a/λ within which the resultant wave vector can fall into the NA circle for a particular propagation direction. The boundary for when this range with four petals pointing in the ΓX direction starts to appear can be determined by the relation $k = |G_{\Gamma X} - NA|$ to be $a/\lambda = 1/(n+NA)$. For further increase of a/λ, the resultant wavevector will leave the NA circle as shown Fig. 9(c).

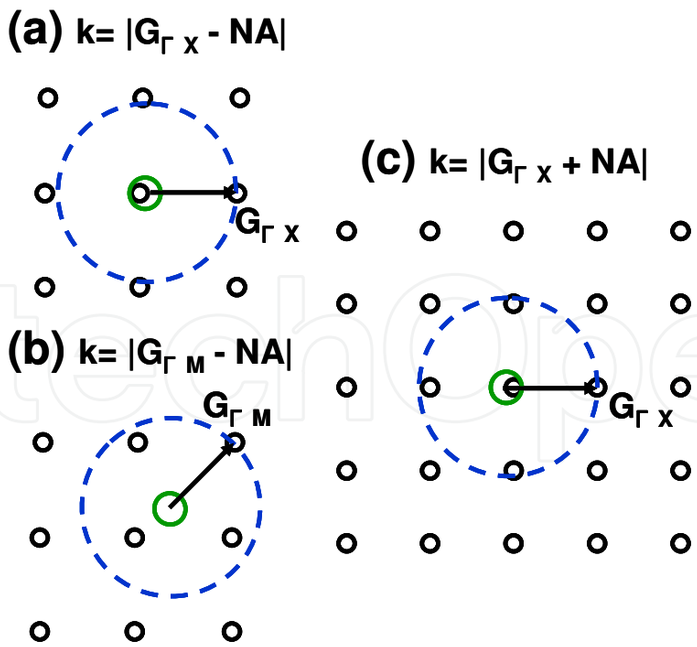

Fig. 9. Ewald constructions for a/λ increases above the cutoff and just start to couple with the shortest lattice vector $G_{\Gamma X}$ (a) in the ΓX directions. (b) ΓM direction with the resultant wave vector falling outside the NA circle and will not be seen by the NA=0.32 objective. (c) a/λ increases further as nk_0 just starts to leave the NA circle to disappear from the CCD image.

For larger lattice constants, the escape cone and the guided mode circle become larger relative to the reciprocal lattice. For $a/\lambda > \sqrt{2}/n$, the coupling to $G_{\Gamma M}$ becomes possible and four more petals appears representing four equivalent ΓM directions. For even larger lattice constants, coupling to the third nearest wave vectors is possible and the number of petals increases to 16. These increased coupling possibilities are observed as the increased number of petals in the images. The boundaries separating these regions can be readily derived using the Ewald construction as shown in Fig. 10 along with our observations.

The above discussion considers the simple case of single mode propagation in the waveguide plane. Since the thickness of the epitaxial layer used for the present study is 3 um, the waveguide is multimode. Every mode can couple with different reciprocal vectors to form their own boundaries for a given number of pedals. When plotted on the map, these boundaries will appear as a band of lines. To present these multimode extractions clearly, only the first and the last mode with modes number '*m*' are shown on Fig. 10. The two outermost lines, $G^{+}_{\Gamma X}$ and $G^{m-}_{\Gamma X}$, define the boundary of the possible a/λ's for all the modes that can fall into NA circle after coupling to $G_{\Gamma M}$. The a/λ values shown on the right side of Fig. 10 correspond to the boundaries for NA=1.

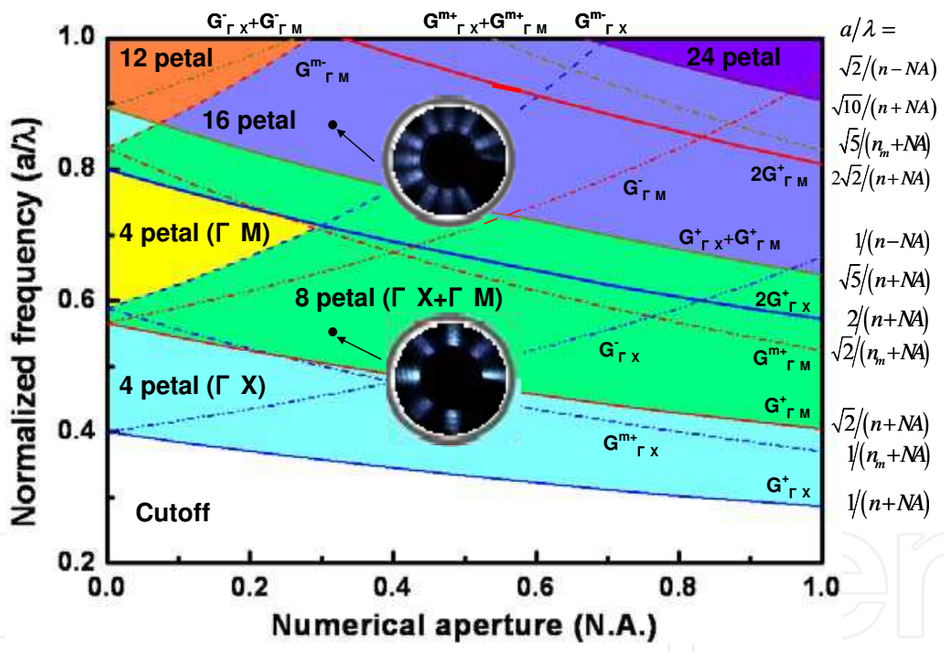

Fig. 10. Map showing regions with different number of petals. The formulas on the right of the figure are the boundary for regions for NA=1. The insets showed the observed 8-fold (a = 260 nm) and 16-fold (a = 410nm) symmetry patterns. The regions of various petals are shown with different colors. The directions of the petals are shown in the parenthesis. The "+" and "-" signs indicate the lower and upper boundary for the regions. The highest mode order number is designated as '*m*' with n_m=1.7 (Sapphire) and the maximum index is n=2.5 (GaN).

In addition, we also observed that the intensity of the light propagating inside the PhC is found to decrease with a decay length of 70-90 μm, depending on the orientation and the

size of the holes. The decay length is determined using the data in the middle dynamic range of the CCD camera where the intensity decay appears as a linear line on the log linear plot. This value is in the same range of that reported in David et al.[17]. Such a parameter is needed for the design of the PhC light extractors.

4. Polarized light emission properties of GaN-based photonic crystal LEDs

Due to valence band intermixing, the side emission of light from quantum well structure is predominantly polarized in the TE direction (along the wafer plane). The observed polarization ratio has been reported to be as high as 7:1 for GaN/InGaN QWs [18]. For common GaN LED structures grown along the *c* axis, access to this polarized light can only be gained by measurements taken from the edge of the sample [19-20]. Several authors have reported polarized light emission for LED structures grown on nonpolar or semipolar GaN substrates [21-22]. In the present study, we investigate the approach employing photonic crystals (PhCs) which do not require the growth on different orientation of sapphire or GaN substrates nor using specific wafer orientations. PhC has been widely studied in recent years [9, 23-26] for the enhancement of LED efficiency, but polarized light emission using PhC has not been investigated. In this section, we use the PhC structure to access the polarized emission and measured their orientation dependence using a specially designed PhC structure to extract the waveguided light. It is found that the PhC can behave as a polarizer to improve the P/S ratio of the extracted EL emission. The results of the P/S ratio for light propagating in different lattice orientation was found to be consistent with the results obtained using the PhC Bloch mode coupling theory [10, 27-28].

4.1 Measurement results

The GaN-based PhC LED samples used in the present work are the same as described before section 3. The polarization properties of the GaN blue PhC LEDs were measured at room temperature using a scanning optical microscopic system, which included continuous wave (CW) current source (Keithley 238), a 20× microscope objective with numerical aperture (NA) = 0.45, a 40× microscope objective with NA = 0.6, and charge-coupled device (CCD) spectrometer with spectral resolution of 0.1 nm. A 20× objective is used to collect the on-axis emission signal from the sample and formed a high-resolution image with a digital camera CCD. Figure 11(a) shows EL CCD image for the sample with square lattice constant a = 260 nm corresponding to a/λ = 0.553. Inset in Fig. 11(a) are the PL CCD image and the reduced Brillioun zone. The observed light emission is from the light propagation along the ΓM and ΓX directions as reported before section 3. Further, the extraction enhancement of the PhC LED chips was determined to be above 100% by mounting the dies on TO packages and using an integration sphere with Si photodiode, when compared to the GaN-based LED chips without PhC. A polarizer (Newport, 10LP-VIS-B) was placed on the GaN blue PhC LEDs for the EL measurements. Figure 11(b) presents CCD image of room temperature EL for samples biased at a drive current of 20 mA. The red dash line indicates the polarization axis for the polarizer. Since the polarization direction of the light is perpendicular to its propagation directions, the light propagated in the direction align with the axis of the polarizer will be blocked. The luminescent signal emitted by the sample was collected by the

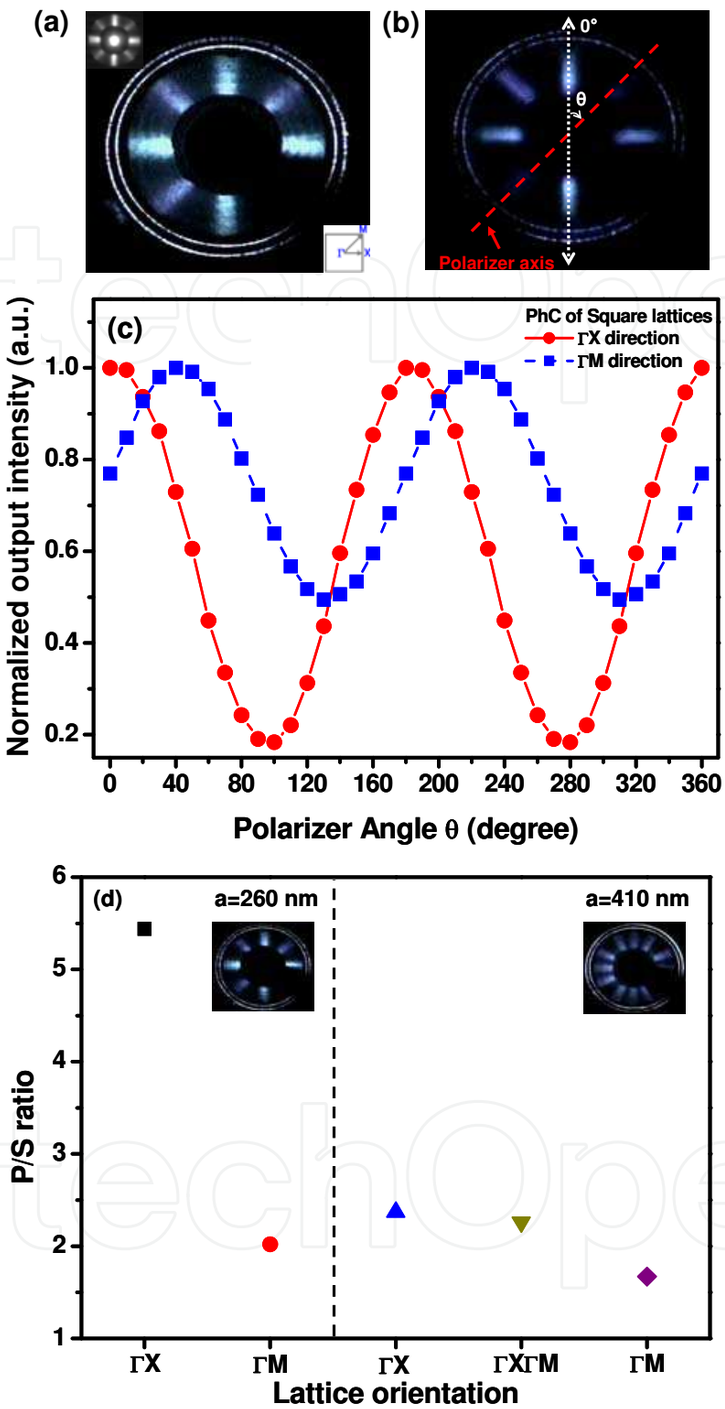

Fig. 11. (a) CCD EL images for lattice constants a = 260 nm, inset of the PL CCD image, and the reduced Brillouin zone. (b) CCD EL images show polarization properties; the red line indicates the polarization axis of the polarizer. (c) Spectrally integrated EL intensity of the GaN PhC LED as a function of polarizer angle θ. (d) *P/S* ratio of different lattice constant as a function of orientation direction.

40× objective lens of the confocal microscope and was transferred to a monochromator for μ-PL measurement through an optical fiber with core diameter of 600 μm. Figure 11(c) shows the EL intensity as a function of the orientation of the polarizing filter placed between the GaN blue PhC LED and the spectrometer, at a drive current of 20 mA. The intensity at various angles was determined from image taken under the same bias condition. Thus the polarization for different propagation direction can be determined as shown in Fig. 11(c). It can be seen that there is a periodic variation of the EL intensity with angular orientation of the polarizer. This indicates that the light collected from the PhC LED is partially polarized, and the P/S ratio [defined as $P/S=I_{max}/I_{min}$] were 5.5 and 2.1 for square lattice (a = 260 nm) in ΓX and ΓM direction, respectively, as shown in Fig. 11(d). Fig. 11(d) also shows the P/S ratio measured in other samples with different period. For square-lattice PhC LEDs, P/S ratio in ΓX orientation is larger than those in other orientations despite the lattice constants. In addition, for the same orientations, PhC LEDs with shorter lattice constant have higher P/S ratio.

4.2 Coupled mode theoretical discussion

The experimental results described above can be explained by examining the electromagnetic field distributions of PhC Bloch modes. Field distributions of Bloch modes were calculated by plane wave expansion (PWE) method using the structure with PhC sandwiched in between air and GaN materials. Figure 12(a) schematically shows the device structure where light is generated and extracted through PhCs. Due to the valence band mixing effects in MQW, guided light propagating in the GaN slab is nearly linear polarized in transverse direction as shown in Fig. 12(b). For PhC a/λ = 0.553, the field distribution for propagation in ΓX and ΓM directions are shown schematically in Fig. 12(c) and Fig. 12(d), respectively, where the arrows indicate the electric field vectors in the plane, and black circles indicate the locations of holes. The individual electric field distributions are complicated, resulting in complicated polarization pattern. It can be seen that the field distribution in ΓX orientation has linear-like polarization behavior, and those in ΓM orientation has circular-like polarization [29]. This behavior can be inferred from the arrangement of the atoms relative to the propagation direction. For ΓX direction, the propagating wave sees the same atom arrangement in the planes perpendicular to the propagating direction from one lattice plane to plane, while in the ΓM direction, the field distribution sees an alternately displaced atom arrangements from plane to plane. Such a staggered atom arrangement will tend to generate the field components normal to the polarization plane. Based on the couple mode theory, the polarization behavior of extracted light can follow the Bloch modes in PhCs and reveal the similar polarization characteristics. Therefore P/S ratio of light extracted through ΓX orientation would be higher than through ΓM orientation. From the Bloch mode patterns in Fig. 12, the experimental polarization results can be realized and consistent with the above discussion.

At a/λ = 0.872, the field distribution in ΓX orientation also has more linear-like than circular-like behavior, and those in ΓM orientation have stronger circular-like polarization as shown in Fig. 12(e) and 12(f). The degree of the polarization appears to be much weaker than that for a/λ = 0.553. In order to discuss this observation, P/S ratio as a function of normalized frequency was calculated. We employ the plane-wave expansion method to calculate the

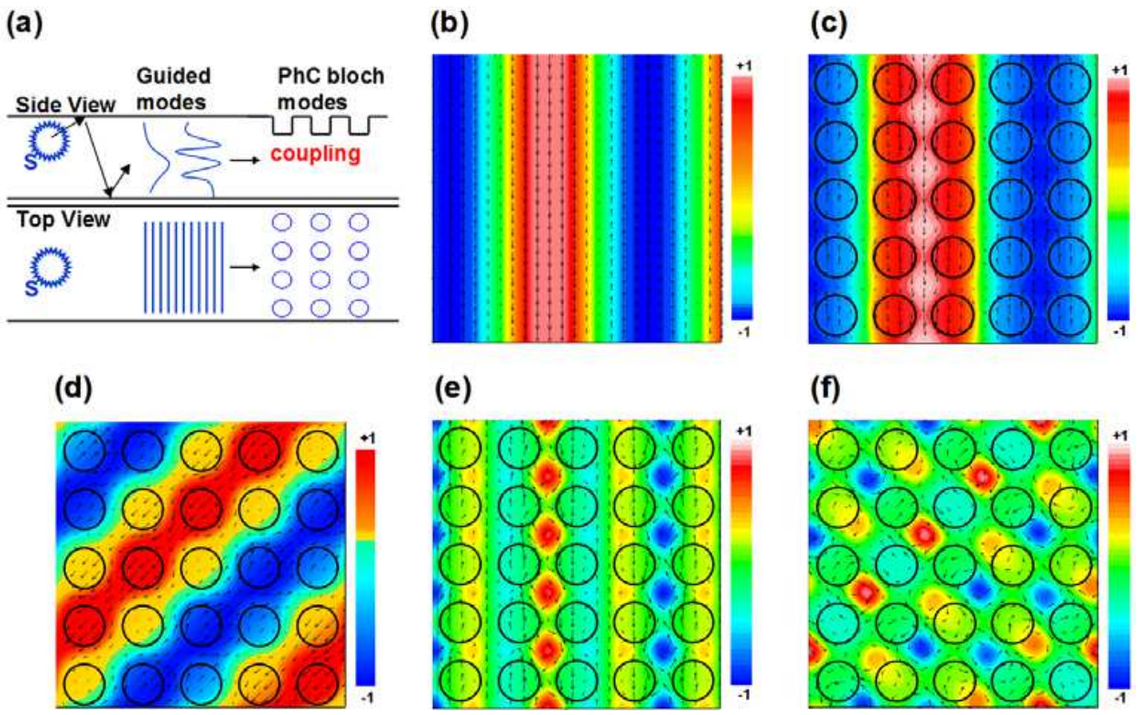

Fig. 12. (a) Schematic of the light generating, propagating, and coupling to PhC Bloch modes. Electromagnetic field distributions for a waveguiding mode in the (b) plane slab guide mode and PhC Bloch modes in the (c) ΓX and (d) ΓM directions of the frequency a/λ = 0.553 and in the (e) ΓX and (f) ΓM directions of the frequency a/λ = 0.872, respectively. Arrows indicate the electric field vectors in the plane, and black circles indicate the locations of lattice points.

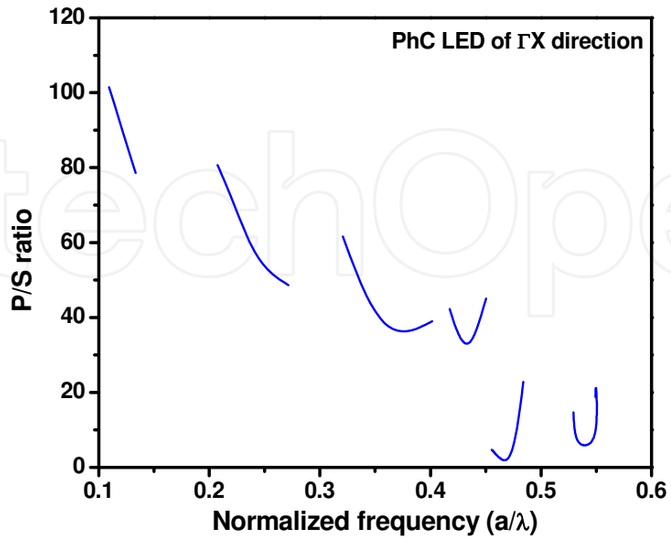

Fig. 13. P/S ratio of PhC Bloch leaky modes in ΓX direction as a function of normalized frequency.

polarization properties (P/S ratio) of the leaky modes in the ΓX directions as a function of normalized frequency. In the calculation, the polarization of the generated light is assumed to be TE polarized. The calculation was carried for each band alone the ΓX direction up to the light line where the light becomes guided and its polarization is then the same as they were generated. As can be seen in Fig. 13, the trend of P/S ratio is decreasing with normalized frequency although the trend within each band is not uniform depending on the filed distribution. Details of this discussion will appear in later publication. It can also be seen from Fig. 13 that by varying the fill factor the lattice constant, the PhC can be designed to have higher extraction efficiency for TE polarization while discriminating the TM polarization. In such case, very high P/S ratio (>10^2) can be achieved. The maximum efficiency for the polarized emission that can be obtained in such case is equal to the TE portion of the total emission which be as high as 88% for a 7:1 P/S ratio.

5. Conclusion

In conclusion, we have experimentally and theoretically demonstrated that surface emitted anisotropic light extraction and polarized light from GaN-based LEDs. The EL images of the anisotropy light extraction distribution in the azimuthal direction were obtained with specially designed annual GaN PhC LED structures, which is dependent on the orientations of the PhC lattice and lattice constants and shows a four-fold symmetric light extraction patterns with varying numbers of petals in the plane of the waveguide. The regions corresponding to the various numbers of petals are determined for increasing lattice constant. More petals appear in the observed image with increasing lattice constant, and some of the petals may disappear. The regions for the appearance and disappearance of the petals are determined by the Bragg diffraction analysis using Ewald construction. In addition the angular dependence of the light extraction for waveguided light incidents to plane with various lattice orientations is also determined. The results show that the light extraction for the square lattices can only occur for certain crystal directions according to the lattice symmetry. Further, a P/S ratio of 5.5 (~85% polarization light) has been observed. The polarization characteristics are theoretically discussed by couple mode theory. At lower normalized frequency, PhC LED has better polarization property, and lattice orientation not only affects the extraction efficiency but also P/S ratio of radiative light. This polarization behavior suggests an efficient means to design and control the GaN blue PhC LEDs for polarized light emission.

6. References

[1] Fujii, T., Gao, Y., Sharma, R., Hu, E. L., DenBaars, S. P., and Nakamura, S. (2004). Increase in the extraction efficiency of GaN-based light-emitting diodes via surface roughening. *Applied Physics Letters*, Vol. 84, pp. 855–857.

[2] Stocker, D. A., Schubert, E. F., and Redwing, J. M. (1998). Crystallorgaphic wet chemical etching of GaN. *Applied Physics Lett.*, Vol. 73, pp. 2654–2656.

[3] Chang, S. J., Chang, C. S., Su, Y. K., Lee, C. T., Chen, W. S., Shen, C. F., Hsu, Y. P., Shei, S. C., and Lo, H. M. (2005). Nitride-based flip-chip ITO LEDs. *IEEE Transactions on Advanced Packaging*, Vol. 28, pp. 273–277.

[4] Wierer, J. J., Steigerwald, D. A., Krames, M. R., O'Shea, J. J., Ludowise, M. J., Christenson, G., Shen, Y. C., Lowery, C., Martin, P. S., Subramanya, S., Gotz, W., Gardner, N. F., Kern, R. S., and Stockman, S. A. (2001). High-power AlGaInN flip-chip light-emitting diodes. *Applied Physics Letters*, Vol. 78, pp. 3379-3381.

[5] Oder, T. N., Kim, K. H., Lin, J. Y., and Jiang, H. X. (2004). III-nitride blue and ultraviolet photonic crystal light emitting diodes. *Applied Physics Letters*, Vol. 84, pp. 466-468.

[6] Wierer, J. J., Krames, M. R., Epoer, J. E., Gardner, N. F., Craford, M. G., Wendt, J. R., Simmons, J. A., and Sigalas, M. M. (2004). InGaN/GaN quantum-well heterostructure light-emitting diodes employing photonic crystal structure. *Applied Physics Letters*, Vol. 84, pp. 3885-3887.

[7] Kim, K., Schubert, E. F., and Cho, J., (2007). Linearly polarized emission from GaInN lightemitting diodes with polarization-enhancing reflector. *Opt. Express*, Vol. 15, pp. 11213-11218.

[8] David, A., Meier, C., Sharma, R., Diana, F. S., DenBaars, S. P., Hu, E., Nakamura, S., and Weisbuch, C. (2005). Photonic bands in two-dimensionally patterned multimode GaN waveguides for light etraction. *Appl. Phys. Lett.*, Vol. 87, pp. 101107-1-101107-3.

[9] Lai, C. F., Kuo, H. C., Chao, C. H., Hsueh, H. T., Wang, J.F. T., Yeh, W. Y., and Chi, J. Y. (2007). Anisotropy of light extraction from two-dimensional photonic crystal light-emitting diodes. *Appl. Phys. Lett.*, Vol. 91, pp. 123117-1-123117-3.

[10] Lai, C. F., Chi, J. Y., Yen, H. H., Kuo, H. C., Chao, C. H., Hsueh, H. T., Wang, J. F. T., Huang, C. Y., and Yeh, W. Y. (2008). Polarized light emission from photonic crystal light-emitting diodes. *Applied Physics Letters*, Vol. 92 No. 24, pp. 243118-1-243118-3.

[11] McGroddy, K., David, A., Matioli, E., Iza, M., Nakamura, S., DenBaars, S., Speck, J. S., Weisbuch, C., and Hu, E. L. (2008). Directional emission control and increased light extraction in GaN photonic crystal light emitting diodes. *Applied Physics Letters*, Vol. 93, pp. 103502-1-103502-3.

[12] Lai, C. F., Chao, C. H., Kuo, H. C., Yen, H. H., Lee, C. E., and Yen, W. Y. (2009). Directional light extraction enhancement from GaN-based film-transferred photonic crystal light-emitting diodes. *Appl. Phys. Lett.*, Vol. 94, pp. 123106-1-123106-3.

[13] Schubert, M.F., Chhajed, S., Kim, J.K., Schubert, E.F. and Cho, J. (2007) Polarization of light emission by 460 nm GaInN/GaN light-emitting diodes grown on (0001) oriented sapphire substrates. *Applied Physics Letters*, Vol. 91, pp. 051117-1-051117-3.

[14] Yeh, P. (1991), *Optical Waves in Layered Media*, Wiley.

[15] Yablonovitch, E. (1987). Inhibited Spontaneous Emission in Solid-State Physics and Electronics. *Physical Review Letters*, Vol. 58, pp. 2059-2062.

[16] Weisbuch, C., David, A., Fujii, T., Schwach, C., Denbaars, S., Nakamura, S., Rattier, M., Bensity, H., Houdre, R., Stanley, R., Carlin, J.F., Krauss, T.F. and Smith, C.J.M. (2004). Recent results and latest views on microcavity LEDs. Proceedings of SPIE, Vol. 5366, pp. 1-19.

[17] David, A., Meier, C., Sharma, R., Diana, F.S., DenBaars, S.P., Hu, E., Nakamura, S. and Weisbuch, C. (2005). Photonic bands in two-dimensionally patterned multimode GaN waveguides for light extraction. *Applied Physics Letters*, Vol. 87, pp. 101107-1-101107-3.

[18] Schubert, M. F., Chhajed, S., Kim, J. K., Schubert, E. F., and Cho, J. (2007). Polarization of light emission by 460 nm GaInN/GaN light-emitting diodes grown on (0001) oriented sapphire substrates. *Appl. Phys. Lett.*, Vol. 91, pp. 051117-1-051117-3.

[19] Shakya, J., Knabe, K., Kim, K. H., Li, J., Lin, J. Y., and Jiang, H. X. (2005). Polarization of III-nitride blue and ultraviolet light-emitting diodes. *Appl. Phys. Lett.*, Vol. 86, pp. 091107-1-091107-3.

[20] Jia, C., Yu, T., Mu, S., Pan, Y., Yang, Z., Chen, Z., Qin, Z., and Zhang, G. (2007). Polarization of edge emission from III-nitride light emitting diodes of emission wavelength from 395 to 455 nm. *Appl. Phys. Lett.*, Vol. 90, pp. 211112-1-211112-3.

[21] Sharma, R., Pattison, M., Masui, H., Farrell, R. M., Baker, T. J., Haskell, B. A., Wu, F., DenBaars, S. P., Speck, J. S., and Nakamura, S. (2005). Demonstration of a semipolar $(10\,\overline{1}3)$ InGaN/GaN green light emitting diode. *Appl. Phys. Lett.*, Vol. 87, pp. 231110-1-231110-3.

[22] T. Koyama, T. Onuma, H. Masui, A. Chakraborty, B. A. Haskell, S. Keller, U. K. Mishra, J. S. Speck, S. Nakamura, and S. P. DenBaars, *Appl. Phys. Lett.*, Vol. 89, pp. 091906, 2006.

[23] Ichikawa, H., and Baba, T. (2004). Efficiency enhancement in a light-emitting diode with a two-dimensional surface grating photonic crystal. *Appl. Phys. Lett.*, Vol. 84, pp. 457-459.

[24] Oder, T. N. , Kim, K. H., Lin, J. Y., and Jiang, H. X., (2004). III-nitride blue and ultraviolet photonic crystal light emitting diodes. *Appl. Phys. Lett.*, Vol. 84, pp. 466-468.

[25] Chen, L., and Nurmikko, A. V. (2004). Fabrication and performance of efficient blue light emitting III-nitride photonic crystals. *Appl. Phys. Lett.*, Vol. 85, pp. 3663-3665.

[26] Lai, C. F., Chi, J. Y., Kuo, H. C., Chao, C. H., Hsueh, H. T., Wang, J.F. T., and Yeh, W. Y. (2008). Anisotropy of light extraction from GaN two-dimensional photonic crystals. *Optics Express,* Vol. 16, pp. 7285-7294.

[27] Lai, C. F., Chi, J. Y., Kuo, H. C., Yen, H. H., Lee, C. E., Chao, C. H., Hsueh, H. T., and Yeh, W. Y. (2009). Far-field of GaN film-transferred green light-emitting diodes with two-dimensional photonic crystals. *Optics Express*, Vol. 17, pp. 8795-8804.

[28] Lai, C. F., Chi, J. Y., Kuo, H. C., Yen, H. H., Lee, C. E., Chao, C. H., Yeh, W. Y., and Lu, T. C. (2009). Far-Field and Near-Field Distribution of GaN-Based Photonic Crystal

LEDs With Guided Mode Extraction. *IEEE. J. Sel. Top. Quant. Electron.*, Vol. 15, pp. 1234-1241.

[29] Imada, M., Chutinan, A., Noda, S., and Mochizuki, M. (2002). Multidirectionally distributed feedback photonic crystal lasers. *Phys. Rev. B*, Vol. 65, pp. 195306-1-195306-8.

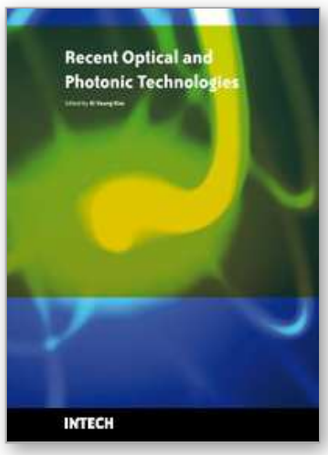

Recent Optical and Photonic Technologies

Edited by Ki Young Kim

ISBN 978-953-7619-71-8
Hard cover, 450 pages
Publisher InTech
Published online 01, January, 2010
Published in print edition January, 2010

Research and development in modern optical and photonic technologies have witnessed quite fast growing advancements in various fundamental and application areas due to availability of novel fabrication and measurement techniques, advanced numerical simulation tools and methods, as well as due to the increasing practical demands. The recent advancements have also been accompanied by the appearance of various interdisciplinary topics. The book attempts to put together state-of-the-art research and development in optical and photonic technologies. It consists of 21 chapters that focus on interesting four topics of photonic crystals (first 5 chapters), THz techniques and applications (next 7 chapters), nanoscale optical techniques and applications (next 5 chapters), and optical trapping and manipulation (last 4 chapters), in which a fundamental theory, numerical simulation techniques, measurement techniques and methods, and various application examples are considered. This book deals with recent and advanced research results and comprehensive reviews on optical and photonic technologies covering the aforementioned topics. I believe that the advanced techniques and research described here may also be applicable to other contemporary research areas in optical and photonic technologies. Thus, I hope the readers will be inspired to start or to improve further their own research and technologies and to expand potential applications. I would like to express my sincere gratitude to all the authors for their outstanding contributions to this book.

InTech Europe
University Campus STeP Ri
Slavka Krautzeka 83/A
51000 Rijeka, Croatia
Phone: +385 (51) 770 447

InTech China
Unit 405, Office Block, Hotel Equatorial Shanghai
No.65, Yan An Road (West), Shanghai, 200040, China
中国上海市延安西路65号上海国际贵都大饭店办公楼405单元
Phone: +86-21-62489820

Fax: +385 (51) 686 166
www.intechopen.com

Fax: +86-21-62489821

IntechOpen